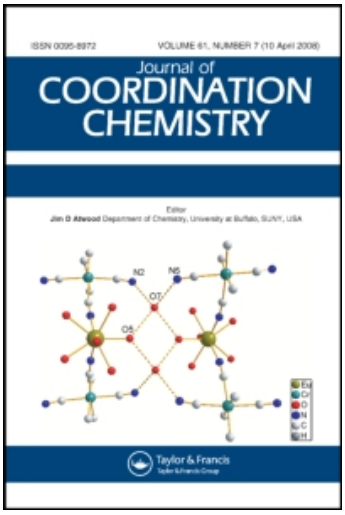

Journal of Coordination Chemistry
Publication details, including instructions for authors and subscription information:
http://www.informaworld.com/smpp/title~content=t713455674

Synthesis, characterization, and DNA interaction of mononuclear copper(II) and zinc(II) complexes having a hard-soft NS donor ligand

N. Raman[a]; R. Jeyamurugan[a]
[a] Research Department of Chemistry, VHNSN College, Virudhunagar-626 001, Tamil Nadu, India

To cite this Article Raman, N. and Jeyamurugan, R.(2009) 'Synthesis, characterization, and DNA interaction of mononuclear copper(II) and zinc(II) complexes having a hard-soft NS donor ligand', Journal of Coordination Chemistry, 62: 14, 2375 — 2387
To link to this Article: DOI: 10.1080/00958970902825195
URL: http://dx.doi.org/10.1080/00958970902825195

Journal of Coordination Chemistry
Vol. 62, No. 14, 20 July 2009, 2375–2387

Taylor & Francis
Taylor & Francis Group

Synthesis, characterization, and DNA interaction of mononuclear copper(II) and zinc(II) complexes having a hard–soft NS donor ligand

N. RAMAN* and R. JEYAMURUGAN

Research Department of Chemistry, VHNSN College,
Virudhunagar-626 001, Tamil Nadu, India

(*Received 22 September 2008; in final form 18 November 2008*)

Knoevenagel condensate-based Schiff base ligands (L) containing N and S donor sites have been designed and synthesized [L = 3-cinnamalideneacetylacetonethiosemicarbazone (CAT)/ 3-cinnamalideneacetylacetoneethylthiosemicarbazone (CAET)/3-cinnamalideneacetylacetone-phenylthiosemicarbazone (CAPT)]. They afford complexes of the type [ML] [M = Cu(II) and Zn(II)]. Both the ligands and their complexes were characterized by analytical and spectral data. Intercalative binding of these complexes with DNA has been investigated by electronic absorption spectroscopy, viscosity measurements, cyclic voltammetry, and differential pulse voltammetry. Electrophoretic study of the complexes indicates that they efficiently cleave supercoiled pUC19 DNA in the presence of hydrogen peroxide.

Keywords: Schiff base; complexes; intercalation; binding constant; nuclease activity

1. Introduction

Coordination chemistry of ligands containing both nitrogen and sulfur as potential donors is of interest, with the most widely studied the thiosemicarbazones [1–5]. Complexes of this type may have biological properties including antitumor [6], antimicrobial [7] properties as well as physicochemical effects [8]. Metal centers bind to proteins and nucleic acids offering cytotoxic effects; coordination compounds and the mechanism of cytotoxic action have been discussed with regard to development of new antitumor agents [9].

Metal complexes interact with the double helix DNA in either a non-covalent or a covalent way. Non-covalent includes intercalation, groove binding, and external static electronic effects; intercalation is one of the most important DNA binding modes as it invariably leads to cellular degradation. It was reported that the intercalating ability increases with the planarity of ligand [10]. Coordination geometry and nature of donors present in the ligand also play key roles in binding of complexes to DNA [11] as does the metal ion type and its valence [12]. Oxidative cleavage of DNA on irradiation with visible light has gained interest due to application in photodynamic therapy [13].

*Corresponding author. Email: drn_raman@yahoo.co.in

Journal of Coordination Chemistry
ISSN 0095-8972 print/ISSN 1029-0389 online
DOI: 10.1080/00958970902825195

Since thiosemicarbazones have beneficial pharmacological properties, we have designed and synthesized modified thiosemicarbazones using Knoevenagel condensate β-diketone and their Cu(II) and Zn(II) complexes to study the interaction of these metal-chelates with DNA. The proposed structures of these ligands and their complexes are shown in scheme 1.

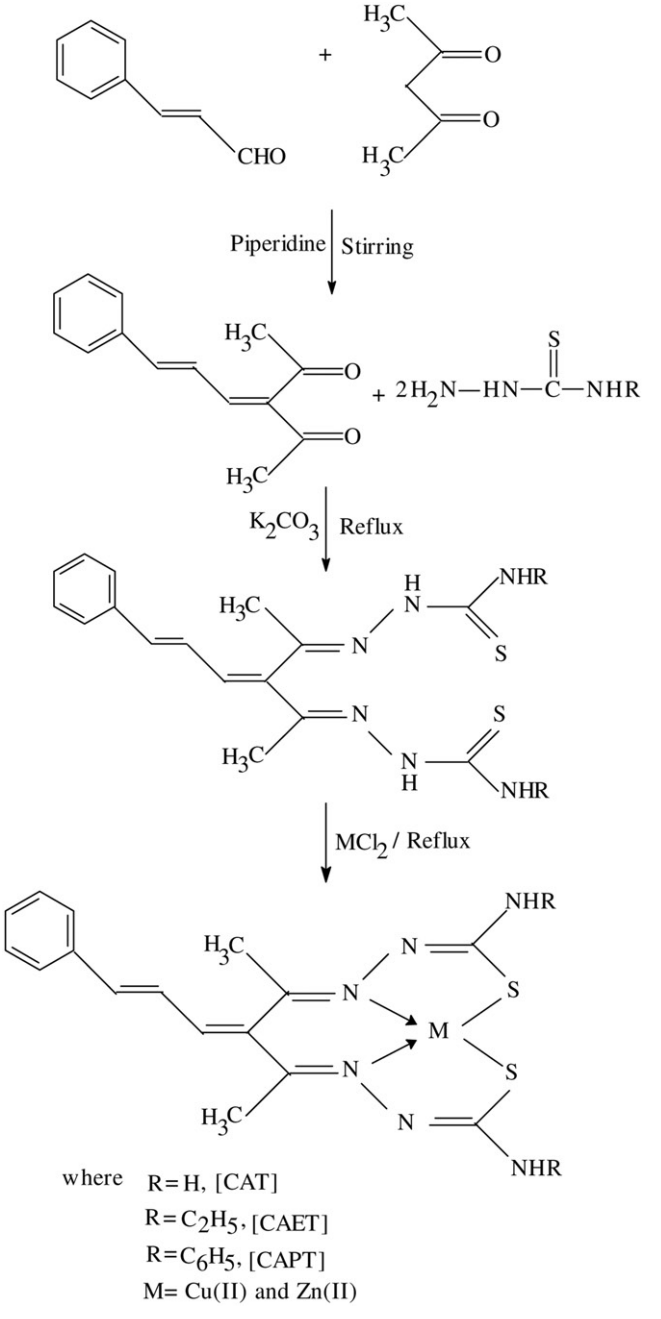

Scheme 1. The outline of the syntheses of ligands and their complexes.

2. Experimental

2.1. *Chemicals*

All reagents and chemicals were purchased from Merck products. Solvents used for electrochemical and spectroscopic studies were purified by standard procedures [14]. Supercoiled pUC19 (cesium chloride purified) DNA was purchased from Bangalore Genei (India). DNA solution in 5 mM *Tris*-HCl/50 mM NaCl (pH 7.2) buffer medium gave a ratio of UV-absorbance at 260–280 nm of *ca* 1.8: 1.9 indicating that the DNA was sufficiently free from protein [15]. The DNA concentration per nucleotide was determined by absorption spectroscopy using the molar absorption coefficient ($6600\,M^{-1}\,cm^{-1}$) at 260 nm [16]. Stock solutions were stored at 4°C and used within 4 days. Agarose (molecular biology grade), ethidium bromide (EB) and tetrabutylammonium perchlorate were obtained from Sigma (USA). *Tris*-HCl buffer solution was prepared using deionized, sonicated triply distilled water.

2.2. *Physical measurements*

Elemental analyzes (C, H, N, and S) were carried out with a Carlo Erba 1108 analyzer. FT-IR spectra of the samples were recorded with a Perkin–Elmer 1800 spectrophotometer from 4000–200 cm^{-1} using KBr pellets. ^{1}H-NMR spectra (300 MHz) of the samples were recorded in $CDCl_3$ and DMSO-d_6 by employing TMS as internal standard on a Bruker Avance DRX 300 FT-NMR spectrometer. Fast atomic bombardment mass spectra (FAB-MS) were obtained using a VGZAB-HS spectrometer in a 3-nitrobenzylalcohol matrix. The X-band ESR spectra of the complexes were recorded at 300 and 77 K using TCNE (tetracyanoethylene) as the *g*-marker. Electronic absorption spectra were recorded using a Shimadzu UV-1601 spectrophotometer. Magnetic susceptibility measurements of the complexes were carried out by Gouy-balance using copper sulfate as the calibrant. The purity of ligands and their complexes was evaluated by column and thin layer chromatography.

Viscosity experiments were carried on an Ostwald viscometer, immersed in a thermostated water-bath maintained at a constant temperature at 30.0 ± 0.1°C. DNA samples of approximately 0.5 mM were prepared by sonicating in order to minimize complexities arising from DNA flexibility [17]. Flow time was measured with a digital stopwatch three times for each sample and an average flow time was calculated. Data were presented as $(\eta/\eta^0)^{1/3}$ versus the concentration of the Cu(II) or Zn(II) complexes, where η is the viscosity of DNA solution in the presence of complex, and η^0 is the viscosity of DNA solution in the absence of complex. Viscosity values were calculated after correcting the flow time of buffer alone (t_0), $\eta = (t - t_0)/t_0$ [18].

Cyclic voltammetry and differential pulse voltammogram studies were performed on a CHI 620C electrochemical analyzer with three electrode system of a glassy carbon (GC) electrode as the working electrode, a platinum wire as auxiliary electrode, and Ag/AgCl as reference electrode. Solutions were deoxygenated by purging with N_2 prior to measurements. The freshly polished GC electrode was modified by transferring a droplet of 2 μL of 5.75×10^{-3} M of DNA solution on to the surface, followed by air drying. Then the electrode was rinsed with distilled water. Thus, a DNA-modified GC electrode was obtained.

The cleavage of pUC19 DNA was determined by agarose gel electrophoresis. The gel electrophoresis experiments were performed by incubation at 37 °C for 2 h of 30 μM pUC19 DNA, 50 μM each complex, and 50 μM H_2O_2 in *Tris*-HCl buffer (pH 7.2). After incubation, samples were electrophoresed for 2 h at 50 V on 1% agarose gel using *Tris*-acetic acid–EDTA buffer (pH 7.2). The gel was then stained using 1 μg cm^{-3} EB and photographed under ultraviolet light at 360 nm. All experiments were performed at room temperature unless otherwise mentioned.

2.3. *Synthesis of CAT*

Knoevenagel condensate β-diketone (3-cinnamalideneacetylacetone) (10 mM, 2.14 g) prepared as per the method adopted by Raman *et al*. [19] was refluxed with an ethanolic solution (30 mL) of thiosemicarbazide (20 mM, 1.82 g) and 1 g of anhydrous K_2CO_3 for 12 h. The solvent was reduced to one-third and the pasty mass so obtained was treated with hot water and set in a refrigerator for 10 h. The solid material formed was removed by filtration and recrystallized from ethanol. Yield: 65%. IR (KBr): 3427 (NH_2), 3237 (N^2H), 1624 (C=N), 789 (C=S) cm^{-1}. ^{1}H-NMR ($CDCl_3$): (phenyl multiplet) 6.4–6.9 δ(m); $\delta(CH_3)$, 2.6 (s); $\delta(NH_2)$, 7.5 (s); δ (N^2H), 10.2 (s). *m*/*z*: 360. Anal. Calcd for $C_{16}H_{20}N_6S_2$: C, 53.3; H, 5.6; N, 23.3; S, 17.8. Found: C, 53.1; H, 5.5; N, 23.0; S, 17.5 (%). λ_{max} in EtOH, 360.5 nm.

Ligands CAET and CAPT were synthesized according to the above described procedure by the replacement of thiosemicarbazide by ethylthiosemicarbazide (2.38 g) and phenylthiosemicarbazide (3.34 g), respectively. Ligand CAET: Yield: 68%. IR (KBr): 3329 (N^4H), 3224 (N^2H), 1618 (C=N), 812 (C=S) cm^{-1}. ^{1}H-NMR ($CDCl_3$): δ(phenyl multiplet), 6.3–6.8 (m); $\delta(CH_3)$, 2.1 (s); $\delta(N^4H)$, 7.4(d); δ (N^2H), 10.3 (s); $\delta(CH_2)$, 3.8 (m); $\delta(CH_3)$ 2.6. *m*/*z*: 417. Anal. Calcd for $C_{20}H_{28}N_6S_2$: C, 57.8; H, 6.8; N, 20.2; S, 15.4. Found: C, 57.5; H, 6.6; N, 20.0; S, 15.1 (%). λ_{max} EtOH, 364 nm. Ligand CAPT: Yield: 64%. IR (KBr): 3316 (N^4H), 3218 (N^2H), 1626 (C=N), 798 (C=S) cm^{-1}. ^{1}H-NMR ($CDCl_3$): δ (phenyl multiplet), 6.2-6.9 (m); $\delta(CH_3)$, 2.6 (s); $\delta(N^4H)$, 7.3 (s); δ (N^2H), 10.2 (s); 2.1. *m*/*z*: 513. Anal. Calcd for $C_{28}H_{28}N_6S_2$: C, 65.6; H, 5.5; N, 16.4; S, 12.5. Found: C, 65.5; H, 5.0; N, 16.0; S, 12.1 (%). λ_{max} in EtOH, 372 nm.

2.4. *Synthesis of [Cu(CAT)]*

An ethanolic solution of CAT (10 mM, 3.61 g) was added to a solution of $CuCl_2$ $2H_2O$ (10 mM, 1.7 g) in ethanol (20 mL) and the mixture was refluxed for 1 h, concentrated to one-third volume and kept at 0°C for 2 h. The solid product formed was filtered, washed several times with small amounts of ethanol and diethyl ether, and dried *in vacuo*. Yield: 64%. IR (KBr): 3422 (NH_2), 1592 (C=N), 612 (C–S), 980 (N–N), 432 (M–N), 374 (M–S) cm^{-1}. *m*/*z*: 422. Anal. Calcd for [$CuC_{16}H_{18}N_6S_2$]: Cu, 15.1; C, 45.5; H, 4.3; N, 19.9; S, 15.2. Found: Cu, 15.0; C, 45.0; H, 4.1; N, 19.4; S, 15.2 (%). λ_M 10^{-3} ($Ohm^{-1}\,cm^2\,mol^{-1}$), 2.1; μ_{eff} (BM), 1.86. λ_{max} in DMF, 386 nm, 520 nm, and 582 nm.

Similarly, [Cu(CAET)] and [Cu(CAPT)] were synthesized according to the above procedure. [Cu(CAET)]: Yield: 61%. IR (KBr): 3326 (N^4H), 1585 (C=N), 619 (C–S), 982 (N–N), 426 (M–N), 386 (M–S) cm^{-1}. *m*/*z*: 479. Anal. Calcd for [$CuC_{20}H_{26}N_6S_2$]: Cu, 13.3; C, 50.2; H, 5.5; N, 17.6; S, 13.4. Found: Cu, 13.0; C, 49.9; H, 5.2; N, 17.2;

S, 13.1 (%). λ_M 10^{-3} ($Ohm^{-1}\,cm^2\,mol^{-1}$), 2.3; μ_{eff} (BM), 1.84. λ_{max} in DMF, 387 nm, 526 nm, and 587 nm. [Cu(CAPT)]: Yield: 58%. IR (KBr): 3326 (N^4H), 1585 (C=N), 619 (C–S), 986 (N–N), 426 (M–N), 386 (M–S) cm^{-1}. *m/z*: 547. Anal. Calcd for [$CuC_{28}H_{26}N_4S_2$]: Cu, 11.6; C, 61.6; H, 4.8; N, 10.3; S, 11.7. Found: Cu, 11.0; C, 61.3; H, 4.5; N, 10.0; S, 11.5 (%). λ_M 10^{-3} ($Ohm^{-1}\,cm^2\,mol^{-1}$), 2.7; μ_{eff} (BM), 1.87. λ_{max} DMF, 389 nm, 528 nm, and 607 nm.

2.5. *Synthesis of [Zn(CAT)]*

A solution of CAT (10 mM, 3.61 g) in ethanol (20 mL) was added to a solution of $ZnCl_2$ (10 mM, 1.36 g) in ethanol (10 mL) and the mixture was refluxed for 1 h, concentrated to one-third volume and kept at 0°C for 2 h. The solid product formed was filtered, washed several times with small amounts of ethanol and diethyl ether, and dried *in vacuo*. Yield: 67%. IR (KBr): 3424 (NH_2), 1589 (C=N), 616 (C–S), 997 (N–N), 437 (M–N), 368 (M–S) cm^{-1}. ^{1}H-NMR ($DMSOd_6$): δ(phenyl multiplet), 6.2–6.8 (m); $\delta(CH_3)$, 2.3 (s); $\delta(NH_2)$, 7.4 (s). *m/z*: 424. Anal. Calcd for [$ZnC_{16}H_{18}N_6S_2$]: Zn, 15.4; C, 45.3; H, 4.3; N, 19.8; S, 15.1. Found: Zn, 15.0; C, 45.0; H, 4.0; N, 19.7; S, 15.0 (%). λ_M 10^{-3} ($Ohm^{-1}\,cm^2\,mol^{-1}$), 1.8. λ_{max} in DMF, 383 nm.

Similarly, for [Zn(CAET)] and [Zn(CAPT)], [Zn(CAET)]: Yield: 62%. IR (KBr): 3328 (N^4H), 1584 (C=N), 627 (C–S), 1002 (N–N), 442 (M–N), 378 (M–S) cm^{-1}. ^{1}H-NMR (DMSO-d_6): δ(phenyl multiplet), 6.8 (m); $\delta(CH_3)$, 2.7 (s); $\delta(N^4H)$, 7.4 (s); $\delta(CH_2)$, 3.7 (m); $\delta(CH_3)$, 2.2. *m/z*: 480. Anal. Calcd for [$ZnC_{20}H_{26}N_6S_2$]: Zn, 13.6; C, 50.1; H, 5.5; N, 17.5; S, 13.4. Found: Zn, 13.2; C, 49.8; H, 5.5; N, 17.3; S, 13.1 (%). λ_M 10^{-3} ($Ohm^{-1}\,cm^2\,mol^{-1}$), 2.3. λ_{max} in DMF, 387.4 nm. [Zn(CAPT)]: Yield: 66%. IR (KBr): 3314 (N^4H), 1590 (C=N), 632 (C–S), 1006 (N–N), 423 (M–N), 387 (M–S) cm^{-1}. ^{1}H-NMR (DMSO-d_6): δ(phenyl multiplet), 6.8 (m); $\delta(CH_3)$, 2.2 (s); $\delta(N^4H)$, 7.4 (d). *m/z*: 576. Anal. Calcd for [$ZnC_{28}H_{26}N6S_2$]: Zn, 11.3; C, 58.4; H, 4.6; N, 14.6; S,11.1. Found: Zn, 11.0; C, 58.0; H, 4.3; N, 14.0; S, 10.7 (%). λ_M 10^{-3} ($Ohm^{-1}\,cm^2\,mol^{-1}$), 1.3. λ_{max} in DMF, 390 nm.

The outline of the syntheses is given in scheme 1.

3. Results and discussion

The ligands and their complexes are stable in air, the ligands are soluble in common organic solvents but their complexes are soluble only in DMF and DMSO. Elemental analyzes of the ligands and their copper and zinc complexes are in agreement with the presented formula. Molar conductivity values indicate that complexes are non-electrolytes.

3.1. *Mass spectra*

The FAB mass spectra of the ligands and complexes were recorded and the obtained molecular ion peaks confirm the proposed formula. The mass spectrum of CAT ligand ($C_{16}H_{20}N_6S_2$) shows triplet peak at 360(M+), 361(M + 1), and 362 (M + 2) with 8.4%, 4.8%, and 2.6% abundances, respectively. The most abundance peak 360 may represent

the molecular ion peak of the ligand. The mass spectrum of its copper complex ($CuC_{16}H_{18}N_6S_2$) shows triplet peak at 422 (M+), 423 (M+1) and 424 (M+2) with 9.3%, 5.7%, and 3.2% abundances, respectively. The one at 422 may represent the molecular ion peak of the complex and the other peaks are isotopic species. The m/z of all the fragments of ligands and their complexes with the relative intensities confirm the stoichiometry of the complexes is being of the type [ML]. Thus, the mass spectral data reinforce the conclusion drawn from the analytical and conductance values.

3.2. *Infrared spectra*

In all the complexes, the $\nu(N^2H)$ band, originally present in the ligand system at 3218–3237 cm^{-1}, disappears and a new band appears at 1618–1624 cm^{-1} due to ν(C=N). The ν(C=N) in the ligand is shifted to lower frequency by *ca* 20 cm^{-1} on complexation [20] and a new band at 423–442 cm^{-1} is assigned to ν(M–N) [21]. The absence of thioamide band ν(HN–C=S) at *ca* 785–815 cm^{-1} and the appearance of a new band at *ca* 612–632 cm^{-1} confirm the conversion of ν(C=S) into ν(C–S) [22]; a new band around 368–387 is assigned to ν(M–S). The reduction of thioamide ν(N=C–SH) observed at *ca* 980 cm^{-1} suggests that coordination occurs through sulfur. These data reveal that the ligands are tetradentate coordinated to the metal ions through the azomethine nitrogens and thiolate sulfurs.

3.3. *Electronic absorption spectra*

The electronic absorption spectra of the Cu(II) complexes recorded in DMF show two bands in the visible region, around 17,500–16,500 and 19,300–18,500 cm^{-1}, assigned to $^2B_{1g} \rightarrow {}^2A_{1g}$ and $^2B_{1g} \rightarrow {}^2E_g$ transitions, respectively, suggesting square-planar geometry around Cu(II). The observed magnetic moments of the Cu(II) complexes (1.84–1.87 B.M) indicate the monomeric nature of the complexes. The electronic absorption spectra of the Zn(II) complexes show the bands (26,000–25,600 cm^{-1}) assigned to intra-ligand charge transfer transitions [23].

3.4. *Nuclear magnetic resonance spectral studies*

The ^{13}C and ^1H-NMR spectra of CAPT and its zinc complex were recorded in $CDCl_3$ and DMSO-d_6, respectively. From ^{13}C-NMR spectral data (table 1), for the zinc complex, the signal for the C–S carbon appears at $\delta = 187.3$ ppm compared with $\delta = 179.2$ ppm in the free ligand (C=S), confirming coordination of thiolate (C–S) to zinc(II) [24]. The deprotonation of the ligand is confirmed by the absence of a resonance attributed to the hydrazinic proton (N^2H) in the ^1H-NMR spectra of the complex which is readily detectable in the spectra of the free ligand at $\delta = 10.3$ ppm.

3.5. *ESR spectra*

ESR spectra of copper(II) complexes were recorded in DMSO at 300 and 77 K. The 300 K spectrum shows an isotropic pattern, expected for Cu^{2+}, but the spectra for the frozen solutions show the usual anisotropic pattern expected for powder sample.

Table 1. ^{13}C-NMR spectral data (ppm) of ligand (CAPT) and its Zn(II) complex.

Assignment	Ligand (CAPT)	[Zn(CAPT)]
C_1	127.7	129.6
C_2	129.1	130.6
C_3	130.5	131.3
C_4	132.1	133.1
C_5	138.4	140.5
C_6	142.3	143.4
C_7	149.2	150.1
C_8	95.7	96.9
C_9	196.2	197.5
C_{10}	27.21	29.8
C_{11}	187.3	179.2
C_{12}	134.6	136.8
C_{13}	129.6	128.3
C_{14}	128.4	127.9
C_{15}	153.4	152.8

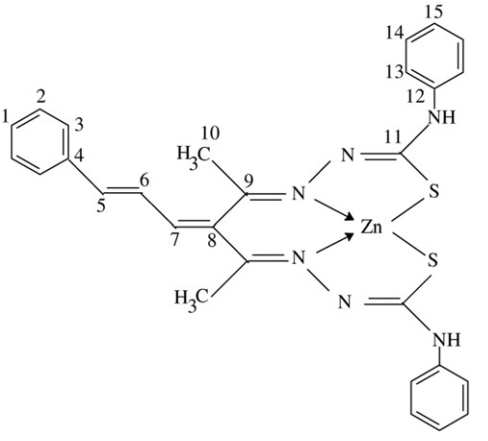

Table 2. Spin Hamiltonian parameters of Cu(II) complexes in DMSO at 300 K and 77 K.

	g-tensor			$A \times 10^{-4}$ (cm^{-1})					
Complexes	$g_\parallel$	$g_\perp$	g_{iso}	$A_\parallel$	$A_\perp$	A_{iso}	α^2	β^2	G
[Cu(CAT)]	2.27	2.04	2.17	158.2	46.5	83	0.75	1.00	7.1
[Cu(CAET)]	2.21	2.03	2.19	152.5	38.3	85	0.68	0.88	7.5
[Cu(CAPT)]	2.34	2.05	2.14	163.1	52.8	80	0.85	1.13	7.0

The absence of half field signal at 1600 G, corresponding to the $\Delta Ms = \pm 2$ transition, rules out any Cu–Cu interaction in the ESR spectra [25]. The spin Hamiltonian parameters of the complexes are given in table 2. The frozen DMSO solution is axial with $g_\parallel > g_\perp > 2.0023$, indicating a $d_{x^2-y^2}$ ground state [26] in agreement with the electronic absorption spectroscopic assignments. The frozen solution spectrum of the complex shows four-line hyperfine splitting $A_\parallel$ with signals penetrating to ^{63}Cu and ^{65}Cu slightly resolved at the low field component. The most remarkable feature is that the $g_\parallel$ value (2.21–2.34) is substantially higher than the majority of known copper(II) complexes [27]. A factor potentially contributing to increase of $g_\parallel$ is distortion from square-planar geometry [28].

The geometrical distortion was ascertained by $g_\parallel/A_\parallel$ ($A_\parallel$ in cm^{-1}) with values less than 140 associated with the square-planar structures, whereas higher values indicate distortions towards tetrahedral [29]. For the present complexes, the $g_\parallel/A_\parallel$ is 143–145 indicating some deviation from planarity which is further confirmed by α^2 whose value is less than unity. The electron spin resonance and optical spectra have been used to determine the covalent bonding parameters for the Cu(II) ion in various ligand fields. We adopted simplified molecular orbital theory [30] to calculate the bonding coefficients, in-plane π-bonding (β^2), out-of-plane π-bonding (γ^2), and in-plane σ-bonding (α^2). The observed α^2 (less than unity) and β^2 (greater than 0.5) values indicate that the present copper(II) complexes have some covalent character.

The observed value for the exchange interaction parameters for the copper complexes ($G = 7.0$–7.5) suggest that weak ligand field and the local tetragonal axes are aligned parallel or slightly misaligned, the unpaired electron is present in the $d_{x^2-y^2}$ orbital [31] and exchange coupling is not operative in the present complexes.

3.6. *Cyclic voltammetry*

Cyclic voltammogram of the complex [Cu(CAPT)] was recorded in DMF solution with tetrabutylammonium perchlorate as the supporting electrolyte. The cyclic voltammogram of the complex (Supplementary material) showed two quasi-redox couples. In the reduction process, it showed a cathodic peak at 0.211 V for $Cu^{III} \rightarrow Cu^{II}$ ($E_{pa} = 0.484$ V, $E_{pc} = 0.211$ V, $\Delta E_p = 0.273$ V, and $E_{1/2} = 0.398$ V). It also showed a cathodic peak at -0.951 V for $Cu^{II} \rightarrow Cu^{I}$ ($E_{pa} = -0.457$ V, $E_{pc} = -0.951$ V, $\Delta E_p = 0.494$ V, and $E_{1/2} = -0.704$ V) reduction, consistent with mononuclear complex [32].

Based on the above spectral and analytical data, the structures of the macrocyclic Schiff-base complexes are shown in scheme 1.

3.7. *DNA binding experiments*

3.7.1. Electronic absorption spectral studies. Absorption titration experiments were carried out by varying the DNA concentration (0–100 μM) and maintaining the metal-complex concentration constant (30 μM). Absorption spectra were recorded after each successive addition of DNA and equilibration (~10 min). The observed data were then fitted into equation (1) to obtain the intrinsic binding constant, K_b [27]:

$$[DNA]/(\varepsilon_a - \varepsilon_f) = [DNA]/(\varepsilon_b - \varepsilon_f) + 1/K_b(\varepsilon_b - \varepsilon_f) \quad (1)$$

where [DNA] is the concentration of DNA in base pairs, ε_a, ε_f, and ε_b are the apparent, free, and bound metal complex extinction coefficients, respectively; K_b is the equilibrium binding constant.

The Cu(II) and Zn(II) complexes bound to DNA through intercalation are characterized by change in absorbance (hypochromism) and blue shift in the wavelength, due to intercalation involving a stacking interaction [33]. The electronic absorption spectra of the complexes in the presence and absence of DNA were monitored at a wavelength of around 350–390 nm. Upon addition of incremental amounts of DNA, a considerable drop in the absorptivity was observed with a moderate shift in absorption wavelength (1–6 nm) (Supplementary material). The change in absorbance values with increasing amount of DNA was fitted into equation (1) to evaluate the intrinsic binding constant K_b (table 3), which for these complexes is of the order of 10^4.

3.7.2. Viscosity measurements. As a means of further clarifying the binding of these complexes to DNA, viscosity measurements were carried out on DNA by varying the concentration of the complexes. Spectroscopic data provide necessary, but not sufficient, clues to support a binding mode. Viscosity measurements, sensitive to DNA length, are the least ambiguous and most critical tests of the binding model in the

Table 3. Absorption spectral properties of Cu(II) and Zn(II) complexes.

Complexes	λ_{max} Free	λ_{max} Bound	$\Delta\lambda$ (nm)	H%	$K_b \times 10^4$ (M^{-1})
[Zn(CAT)]	383.5	378.6	2.4	7	1.4
[Cu(CAET)]	387.0	383.6	4.7	12	2.4
[Zn(CAET)]	379.4	376.0	2.7	8	1.3
[Cu(CAPT)]	389.0	383.6	5.7	17	3.2
[Zn(CAPT)]	390.0	386.5	3.1	11	2.1

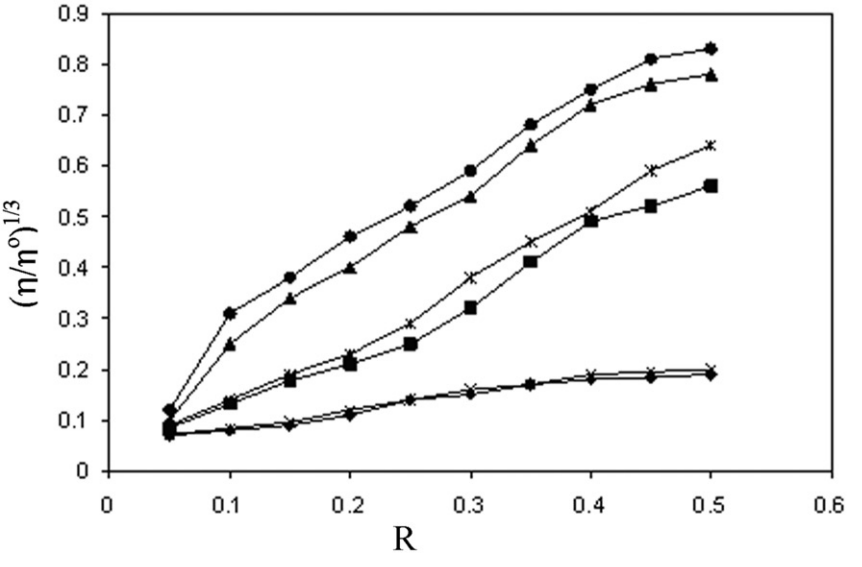

Figure 1. The effect of [Zn(CAT)] (×), [Zn(CAET)] (*) , [Zn(CAPT)] (●) , [Cu(CAT)] (♦) , [Cu(CAET)] (■), and [Cu(CAPT)] (▲) on the viscosity of DNA; relative specific viscosity *vs.* R = $[CuL^{2+}]$/[DNA] or $[ZnL^{2+}]$/[DNA].

absence of crystallographic structural data [34]. A classical intercalative mode causes a significant increase in viscosity of the DNA solution in the presence of complexes due to an increase in separation of base pairs at the intercalation sites and hence an increase in overall length. In contrast, groove-face or electrostatic interactions typically cause less pronounced (positive or negative) or no change in the DNA solution viscosity [27]. A partial or nonclassical intercalation of the ligand would reduce the DNA viscosity [35]. Values of $(\eta/\eta^0)^{1/3}$ were plotted against $[CuL]^{2+}$/[DNA] or $[ZnL]^{2+}$/[DNA] in the absence and presence of the copper or zinc complexes. The results indicate that the present Cu(II) and Zn(II) complexes increase the viscosity of the DNA solutions (figure 1). Therefore, it is apparent that the complexes bind to double-stranded DNA by intercalation.

3.7.3. Electrochemical studies. Cyclic and differential pulse voltammetric techniques are useful in probing the nature and mode of DNA binding of metal complexes.

Typical cyclic voltammogram of [Cu(CAPT)] in the absence and in presence of varying amounts of [DNA] are provided in Supplementary material.

In the absence of DNA, the first redox couple cathodic peak appears at 0.211 V for $Cu^{III} \rightarrow Cu^{II}$ ($E_{pa} = 0.484$ V, $E_{pc} = 0.211$ V, $\Delta E_p = 0.273$ V, and $E_{1/2} = 0.398$ V) and second redox couple cathodic peak appears at −0.951 V for $Cu^{II} \rightarrow Cu^{I}$ ($E_{pa} = -0.457$ V, $E_{pc} = -0.951$ V, $\Delta E_p = 0.494$ V, and $E_{1/2} = -0.704$ V). These two redox couples ratio of $i_{pc} : i_{pa}$ is approximately unity, indicating that reaction of the complex on the glassy carbon electrode surface is quasi-reversible. Incremental addition of DNA to the complex causes a negative shift in $E_{1/2}$ of 46 mV and a decrease in ΔE_p of 14 mV for the second redox couple. The i_{pc}/i_{pa} values also decrease in the presence of DNA. The decrease of the anodic and cathodic peak currents of the complex in the presence of DNA is due to decrease in the apparent diffusion coefficient of the Cu(II) complex upon complexation with the DNA macromolecules. These results show that [Cu(CAPT)] stabilizes the duplex (GC pairs) by intercalation. The first redox couple of [Cu(CAPT)] shows no significant change of potential or intensity of currents, indicating that the first redox couple species does not stabilize duplex DNA.

Zn(II) complexes show only the oxidation peak from −1.08 to −1.14 V (E_p) and no reduction peak in the absence of DNA. Incremental addition of DNA to Zn(II) complexes shows a decrease in the current intensity and negative shift of the oxidation peak potential, demonstrating interaction between Zn(II) and DNA. The electrochemical parameters of the Cu(II) and Zn(II) complexes are shown in tables 4 and 5, respectively. These data indicate that all the synthesized Cu(II) and Zn(II) complexes interact with DNA through intercalation.

Differential pulse voltammogram of [Cu(CAPT)] (Supplementary material) show that an increase in concentration of DNA causes a negative potential shift along with significant decrease of current intensity. The shift in potential is related to the ratio of binding constant,

$$E_b^{0\prime} - E_f^{0\prime} = 0.0591 \log (K_+/K_{2+}) \quad (2)$$

Table 4. Electrochemical parameters for interaction of DNA with Cu(II) complexes.

	$E_{1/2}$ (V)		ΔE_p (mV)			
Complexes	Free	Bound	Free	Bound	K_+/K_{2+}	i_{pc}/i_{pa}
[Cu(CAT)]	−0.556	−0.534	426	413	0.84	0.75
[Cu(CAET)]	−0.624	−0.594	454	442	0.95	0.84
[Cu(CAPT)]	−0.704	−0.658	494	478	0.95	0.92

Table 5. Electrochemical parameters for interaction of DNA with Zn(II) complexes.

	E_p (V)		I_p (A)		
Complexes	Free	Bound	Free	Bound	$K_d \times 10^{-10}$ (mol L^{-1})
[Zn(CAT)]	−0.54	−0.52	0.42	0.38	1.07
[Zn(CAET)]	−0.56	−0.53	0.36	0.24	2.4
[Zn(CAPT)]	−0.57	−0.55	0.41	0.32	2.6

where $E_b^{0\prime}$ and $E_f^{0\prime}$ are formal potentials of the Cu(II)/Cu(I) complex couple in the bound and free form, respectively. The ratio of the binding constants (K_+/K_{2+}) for DNA binding of Cu(II)/Cu(I) complexes were found to be less than unity (table 4), indicating that binding of Cu(I) complex to DNA is small compared to that of Cu(II) complex. The experimental results indicate the preferential stabilization of Cu(II) over Cu(I) on binding to DNA. The possible mechanism is shown below:

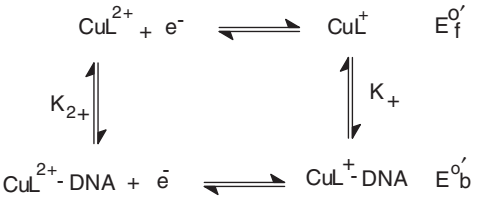

Differential pulse voltammogram of the present Zn(II) complexes gave a negative potential shift along with significant decrease of current intensity during addition of DNA, indicating that zinc ions stabilize the duplex (GC pairs) by intercalation. Hence, the electrochemical reduction reaction can be divided into two steps:

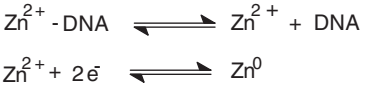

The dissociation constant (K_d) of the Zn(II)-DNA complex was obtained using the following equation:

$$i_p^2 = \frac{K_d}{[\mathrm{DNA}]}\left(i_{p0}^2 - i_p^2\right) + i_{p0}^2 - [\mathrm{DNA}] \tag{3}$$

where K_d is dissociation constant of Zn(II)-DNA, i_{p0}^2 and i_p^2 are reduction current of Zn(II) in the absence and presence of DNA, respectively. Using equation (3), the dissociation constant was determined (figure 2). The low dissociation constant values (table 5) of Zn(II) ions were indispensable for catalytic function and structural stability of zinc enzymes which participate in the replication, degradation, and translation of genetic material of all species. Moreover, Zn(II) ions were probably interacting not only with the active site of the enzyme during these processes, as already known in the literature [36], but also with DNA.

3.7.4. Cleavage of pUC19 DNA. Gel electrophoresis using pUC19 DNA was performed with ligands and their complexes in the presence and absence of H_2O_2. At micromolar concentrations for 2 h incubation periods, the ligands exhibit no significant activity in the presence of oxidant (H_2O_2). Nuclease activity is greatly enhanced by incorporation of metal ion in the ligand. The complexes cleave DNA more efficiently in the presence of oxidant, which may be attributed to the formation of hydroxyl free radical. The production of a hydroxyl free radical due to reaction between the metal complexes and oxidant may be explained as shown below [37].

$$M^{n^+} + H_2O_2 \rightarrow M^{(n+1)^+} + HO^{\bullet} + HO^-$$

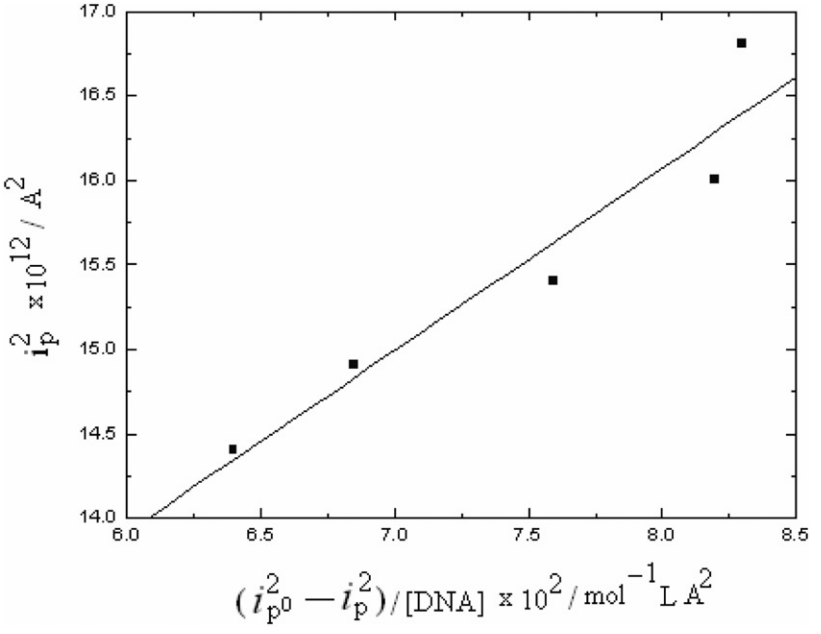

Figure 2. Determination of the dissociation constant of Zn(II)-DNA of the complex, [Zn(CAPT)].

These $HO^{\bullet}$ free radicals participate in the oxidation of deoxyribose moiety, followed by hydrolytic cleavage of the sugar phosphate backbone [38]. The more pronounced nuclease activity of these adducts in the presence of oxidant is due to increased production of hydroxyl radicals. In the absence of oxidant, the metal complexes exhibit no significant DNA cleavage activity due to poor binding of the complexes with DNA, consistent with intercalative binding of complexes with DNA through the minor groove because complexes containing ligands of increasing hydrophobicity which are not planar favor minor groove binding [39].

4. Conclusions

Knoevenagel condensate-based Schiff base complexes of Cu(II) and Zn(II) containing hard-soft NS donor ligands have been designed, synthesized, and characterized by analytical and spectral methods. The intercalative binding of the complexes with DNA has been supported by electronic absorption spectra, cyclic voltammetry, differential pulse voltammetry, and viscometric studies. The complexes exhibit nuclease activity in the presence of hydroxyl radicals.

Acknowledgments

The authors gratefully acknowledge the financial support for this work by the Department of Science and Technology, New Delhi, India. They express their heartfelt thanks to the VHNSN College Managing Board for providing the research facilities.

References

[1] Z. Xiao, P.S. Donnelly, M. Zimmermann, A.G. Wedd. *Inorg. Chem.*, **47**, 4338 (2008).
[2] V. Opletalová, D.S. Kalinowski, M. Vejsová, J. Kunes, M. Pour, J. Jampílek, V. Buchta, D.R. Richardson. *Chem. Res. Toxicol.*, **21**, 1878 (2008).
[3] J.S. Casas, M.S. García-Tasende, J. Sordo. *Coord. Chem. Rev.*, **209**, 197 (2000).
[4] G.A.A. Al-Hazmi, M.S. El-Shahawi, A.A. Al-Asmy. *Transition Met. Chem.*, **30**, 464 (2005).
[5] D. Mishra, S. Naskar, M.G.B. Drew, S. Chattopadhyay. *Inorg. Chim. Acta*, **359**, 585 (2006).
[6] Z. Afrasiabi, E. Sinn. *J. Chen. Inorg. Chim. Acta*, **357**, 271 (2004).
[7] N. Raman, A. Kulandaisamy, C. Thangaraja. *Transition Met. Chem.*, **29**, 129 (2004).
[8] E. Labisbal, K.D. Haslow, A. Sousa-Pedrares, J. Valdes-Martınez, S. Hernandez-Ortega, D.X. West. *Polyhedron*, **22**, 2831 (2003).
[9] O.S. Zhukova, IaV. Dobrynin. *Vopr Onkol*, **47**, 706 (2001).
[10] H. Xu, K.C. Zheng, H. Deng, L.J. Lin, Q.L. Zhang, L.N. Ji. *Dalton Trans.*, **3**, 2260 (2003).
[11] H. Xu, K.C. Zheng, H. Deng, L.J. Lin, Q.L. Zhang, L.N. Ji. *New J. Chem.*, **27**, 1255 (2003).
[12] A. Mozaar, S. Elham, R. Bijan, H. Leila. *New J. Chem.*, **28**, 1227 (2004).
[13] K. Szacilowski, W. Macyk, A. Drzewiecka-Matuszek, M. Brindell, G. Stochel. *Chem. Rev.*, **105**, 2647 (2005).
[14] D.D. Perrin, W.L.F Armarego, D.R. Perrin. *Purification of Laboratory Chemicals*, Pergamon Press, Oxford (1980).
[15] J. Marmur. *J. Mol. Biol.*, **3**, 208 (1961).
[16] M.E. Reichmann, S.A. Rice, C.A. Thomas, P. Doty. *J. Am. Chem. Soc.*, **76**, 3047 (1954).
[17] J.B. Charies, N. Dattagupta, D.M. Crothers. *Biochemistry*, **21**, 3933 (1982).
[18] S. Satyanarayana, J.C. Daborusak, J.B. Charies. *Biochemistry*, **32**, 2573 (1983).
[19] N. Raman, C. Thangaraja. *Transition Met. Chem.*, **30**, 317 (2005).
[20] S.K. Sengupta, O.P. Pandey, A. Rai, A. Sinha. *Spectrochim. Acta (A)*, **65**, 139 (2006).
[21] I.T. Ahmed. *Spectrochim. Acta (A)*, **65**, 5 (2006).
[22] G.A. Al-Hazmi, N.M. El-Metwally, O.A. El-Gammal, A.A. El-Asmyb. *Spectrochim. Acta (A)*, **69**, 56 (2008).
[23] A.B.P. Lever. *Inorganic Electronic Spectroscopy*, Elsevier, Amsterdam (1984).
[24] A.R. Cowley, J.R. Dilworth, P.S. Donnelly, J. Woollard-Shore. *Dalton Trans.*, 748 (2003).
[25] A.L. Sharma, I.O. Singh, H.R. Singh, R.M. Kadam, M.K. Bhide, M.D. Sastry. *Transition Met. Chem.*, **26**, 532 (2001).
[26] R.N. Patel, N. Singh, K.K. Shukla, U.K. Chauhan, J. Nicols Gutierrez, A. Castineiras. *Inorg. Chim. Acta*, **357**, 2469 (2004).
[27] C. Oberling, M. Guerin. *Adv. Cancer Res.*, **2**, 353 (1954).
[28] A.W. Addison. In *Copper Coordination Chemistry: Biochemical, Inorganic, Perspectives*, K.D. Karlin, J. Zubieta (Eds), Adenine Press, New York (1983).
[29] A.W. Addison. *Inorg. Chim. Acta*, **162**, 217 (1989).
[30] R.K. Ray, G.B. Kauffman. *Inorg. Chim. Acta*, **173**, 207 (1990).
[31] R. Seangprasertkji, T.L. Riechel. *Inorg. Chem.*, **23**, 991 (1984).
[32] M.C.B. de Oliveira, M. Scarpellini, A. Neves, H. Terenzi, A.J. Bortoluzzi, B. Szpoganics, A. Greatti, A.S. Mangrich, E.M. de Souza, P.M. Fernandez, M.R. Soares. *Inorg. Chem.*, **44**, 921 (2004).
[33] S.A. Tysoe, R.J. Morgan, A.D. Baker, T.C. Strekas. *J. Phys. Chem.*, **97**, 1707 (1993).
[34] B.C. Baguley, M. Lebret. *Biochemistry*, **23**, 937 (1984).
[35] G. Yang, J.Z. Wu, L. Wang, L.N. Ji, X. Tian. *J. Inorg. Biochem.*, **66**, 141 (1997).
[36] G.M. Blackburn, M.J. Gait. *Nucleic Acid in Chemistry and Biology*, 2nd Edn, Oxford University Press, New York (1996).
[37] K. Yamamoto, S. Kawanishi. *J. Biol. Chem.*, **15**, 264 (1984).
[38] P. Merfley, E.R. Robinson. *Mutat. Res.*, **86**, 155 (1981).
[39] H.Y. Mei, J.K. Barton. *J. Am. Chem. Soc.*, **108**, 7414 (1986).